

Density functional theory prediction of a hysteretic phase transition in InPu crystals

Sven P. Rudin

Los Alamos National Laboratory, Los Alamos, New Mexico 87545, USA

(Received 28 April 2008; published 28 May 2008)

Elemental plutonium (Pu) transforms between phases with dramatic changes in volume and symmetry, and a pathway connecting the radically different crystal structures was only recently mapped. Density functional theory calculations presented here predict in the indium-plutonium (InPu) alloy an analogous but structurally much simpler phase transition, characterized by a pairing-up of Pu atoms. The transition connects two crystal structures closely related to the experimentally observed θ -InPu; in one structure, pairing of the Pu atoms breaks the crystal symmetry while the other structure is a trigonal distortion of θ -InPu. The calculations predict these structures to stabilize at low temperatures, where uniaxial strain induces the transition between them. The transition shows hysteresis in the character of the electronic state, in the Pu-Pu bond lengths and in the density.

DOI: [10.1103/PhysRevB.77.172104](https://doi.org/10.1103/PhysRevB.77.172104)

PACS number(s): 61.66.Dk, 64.70.kd, 71.27.+a, 71.28.+d

Temperature drives elemental plutonium (Pu) through structural phase transitions with remarkable features.¹ The solid takes on more crystal structures than any other element—six—and these span a wide range of densities and symmetries. At low temperatures, Pu appears in complex, unique allotropes with low symmetry and high density. The room temperature α phase exemplifies the low symmetry with a monoclinic unit cell containing sixteen atoms. Increased temperatures bring about structures with much higher symmetry and greatly reduced density, e.g., the technologically most important δ phase with face-centered cubic crystal structure.

Considerable research has gone into clarifying the particulars of the phase transitions with mixed success. In particular, the details of a pathway connecting the crystal structures was only recently identified due to the vastly different symmetries.² Recent theory predicts that imposing structural constraints could abate the geometric complexity of the phase transitions.³ The suggested constraint involves alternating nanometer-scale layers of Pu and lead (Pb). The Pb layer imparts its high degree of symmetry on the Pu layer, which reduces the intricate phase transitions of elemental Pu to a simple change of geometry: a pairing up of neighboring Pu planes akin to atoms in the one-dimensional Peierls effect.⁴

Many of the remarkable traits of elemental Pu's phase transitions remain in the geometrically simpler transition. For one, the density changes by a large amount. Then, quite surprisingly, the Pu-Pu bond lengths in the unpaired phase closely approximate the bond length in δ -Pu, while in the paired phase they emulate the α phase by separating into sharply defined groups of short or long bonds. Most importantly, the character of the $5f$ electron states transforms as markedly as in elemental Pu.

The simplicity of the transition's geometry has allowed a more detailed theoretical exploration of the accompanying changes in electronic states than previously possible.⁵ Density functional theory⁶ (DFT) calculations reveal that stepping through the transition, i.e., smoothly pairing up Pu planes, steadily changes the character of the $5f$ electron states. This path between the unpaired and paired phases takes the system over an energy maximum. These results suggest that when Pu undergoes a transition from one phase

to the other, any sudden change in the character of the electronic states correlates with a sudden change in geometry and vice versa.

Experimental verification of the predicted behavior in Pb-Pu superlattices would first require their successful fabrication. In the work presented here, theory predicts that a similarly simplified version of the phase transition emerges in the θ -phase of the indium-plutonium (InPu) alloy, a system which already has been successfully created in the laboratory.⁷ The transition distinguishes itself by a pairing up of Pu atoms, which the calculations predict to be observable at low temperatures and influenceable by uniaxial strain.

The source of Pu's striking solid-state attributes also poses a challenge to theory. DFT works well for most other elements in the approximations used to make the theory practical, i.e., the local density approximation⁸ and the generalized gradient approximation (GGA).⁹ While DFT in the GGA describes the α -Pu phase well, it fails to describe the δ -Pu phase. The failure plausibly stems from a varying localization of the $5f$ electronic states.¹⁰⁻¹³ To make up for this, sophisticated alternatives to the approximate implementation of DFT have been designed. The purpose-built methods for handling the $5f$ electron states include the mixed level model¹⁴ and dynamical mean field theory.¹⁵

A simpler but effective approach to account for the changing character of the $5f$ electron states arises from DFT calculations in the GGA that allow spin polarization.^{12,16-19} This approach reliably replicates the equilibrium structures and energetics of Pu compounds²⁰ and Pu alloys,^{21,22} and hence serves as an appropriate method of investigating the structure and energetics of InPu. The arising of spin moments reveals one important limitation as no experiment has measured Pu as magnetic.²³ Spin moments arising on the Pu atoms thus should not be viewed as predicted magnetic moments but merely as indication of the changing character of the $5f$ electron states.

All results presented here stem from calculations using the Vienna *ab initio* simulation package^{24,25} (VASP) and their only crucial difference to those on Pb-Pu superlattices^{2,5} is the replacement of the Pb potential with that designed for In. Supplied with VASP, this projector-augmented wave²⁶ potential treats as valence electrons the $5s$ and $5p$ valence states, the remaining electrons remain frozen in atomic core states.

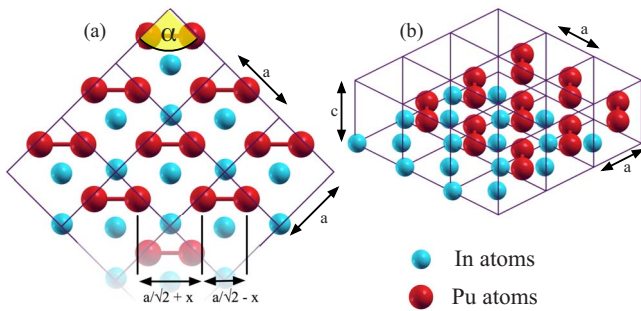


FIG. 1. (Color online) Geometry of the predicted InPu ground state crystal structure. (a) Top view and (b) perspective view of nine unit cells. The calculated equilibrium values are $a=4.48$ Å, $c=4.88$ Å, and $x=0.62$ Å. Pairing of the Pu atoms (indicated by bonds) slightly distorts the In sublattice by displacing the In atoms horizontally by 0.23 Å away from the Pu pairs (particularly evident in the perspective view).

For Pu, the valence electrons include the 6s and 6p semicore (because of the arising short Pu-Pu bonds) and the 5f, 6d, 7s, and 7p valence states. Exchange and correlation are treated in the GGA with the functional of Perdew and Wang^{27,28} (PW91). For the four-atom unit cell, an $8 \times 8 \times 10$ k -point mesh converges the total energy (calculated using the linear tetrahedron method with Blöchl corrections²⁹) within 1 meV/atom. The same convergence criteria for energy differences arise with the plane wave energy cut-off of 320 eV.

The experimentally determined θ -InPu phase exists between room temperature and melting (at 1145 °C) as a AuCu type crystal structure (Strukturbericht designation L1₀, Pearson symbol tP2) with lattice constants 4.81 and 4.54 Å.⁷ Figure 1 illustrates the closely related InPu ground state crystal structure predicted by DFT in the GGA. This structure differs from the experimental lattice by a pairing of Pu atoms and a slight displacement of the In atoms (away from the paired Pu atoms). These changes double both basal plane dimensions. The calculated lattice constants of $a=4.48$ Å and $c=4.88$ Å disagree somewhat with the experimentally measured values and invert the c/a ratio. Relative to α -Pu and the face-centered tetragonal In ground state, the structure has a calculated energy of mixing of 144 meV (neglecting zero-point energy and thermal contributions).

The pairing of Pu atoms brings them closer by $x=0.62$ Å. Figure 2 shows the double well produced for pairing as a function of the parameter x . The same double well exists for pairing in the perpendicular direction within the basal plane. The well depth of 31 meV only slightly exceeds the energy corresponding to room temperature, 27 meV, suggesting that at 300 K, the system can easily tunnel through the barrier, and the average atomic positions would show no pairing. In the experiments of Ellinger *et al.* no evidence for pairing was seen above room temperature.⁷ However, the energy scale of the double wells suggests that at lower temperatures, the system could become trapped in one of the four possible arrangements with paired Pu atoms.

Further calculations predict the existence of a metastable geometry without paired Pu atoms, as illustrated in Fig. 3. This unpaired phase differs from the experimental lattice by

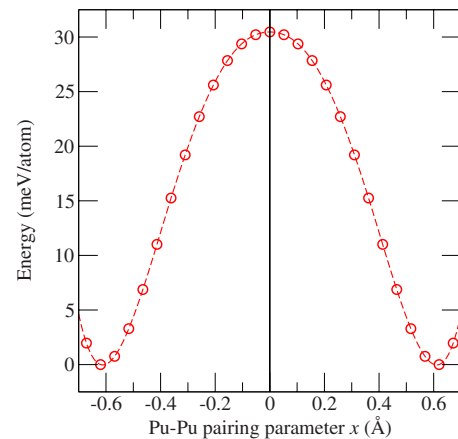


FIG. 2. (Color online) Calculated energy per atom plotted against the parameter measuring the pairing of Pu atoms. Circles represent the calculated energies, connected by a spline to guide the eye. The simulation cell is kept fixed at $a=4.48$ Å, $c=4.88$ Å. The In atoms move by proportional amounts.

a trigonal distortion that changes the angle α between basal lattice vectors from 90° to 97.5°. The basal lattice constant a increases to 4.67 Å, while the vertical lattice parameter c decreases slightly to 4.74 Å. The two predicted phases differ in energy by 17.5 meV per atom and in volume by 1.31 Å³ per atom (equivalent to an 11% change per Pu atom, roughly half the difference between the volumes of the α and δ phases of pure Pu). The Pu-Pu bond lengths at $\alpha=90^\circ$ are $a/\sqrt{2}-x=2.55$ Å and $a/\sqrt{2}+x=3.79$ Å, which lie close to the two respective groups of bond lengths in α -Pu (short 2.42–2.53 Å, long 3.21–3.56 Å); in the unpaired phase, the Pu-Pu bond lengths measure 3.52 Å, only slightly larger than those in δ -Pu. In short, the two phases closely emulate the stark structural differences found between the α and δ phases of elemental Pu.

The simplicity of the pathway connecting the two phases allows a prediction of how changing external constraints can induce the phase transition. To this end, quasistatic calculations were performed to optimize the volume, atomic positions, and electronic structure at sequences of fixed values of α . The sequences start with the geometry of one of the two phases. Each step in the succession is initiated with the geometry optimized for the previous value of α , modified by

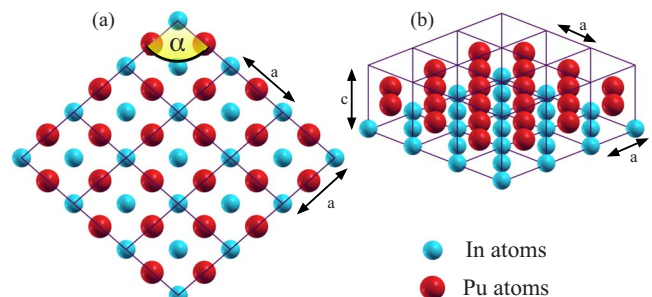


FIG. 3. (Color online) Geometry of the predicted InPu metastable crystal structure. (a) Top view and (b) perspective view of nine unit cells. The calculated equilibrium values are $a=4.67$ Å, $c=4.74$ Å, and $\alpha=97.5^\circ$.

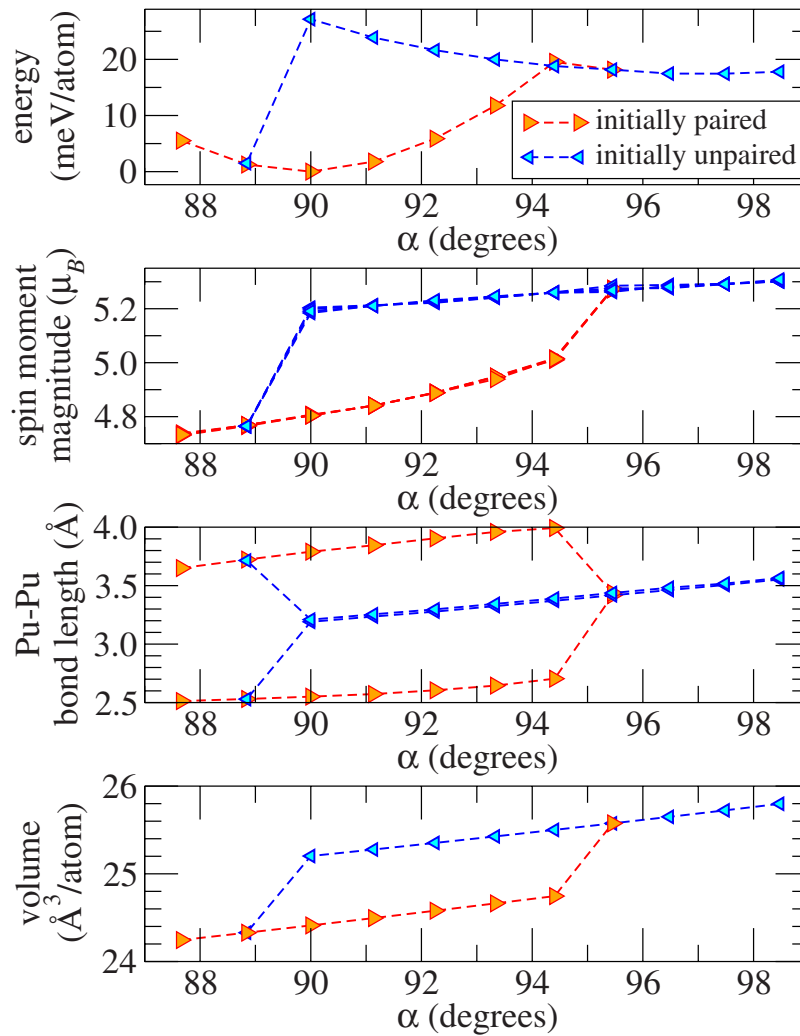


FIG. 4. (Color online) Calculated energy per atom, spin moment magnitude on each Pu atom, Pu-Pu bond length, and volume per atom plotted against the angle α of the trigonal strain of the unit cell. Symbols mark the results obtained for successive values of α , connected by lines to guide the eye. Varying α drives each phase from equilibrium through metastability into the other phase, causing a hysteresis in the electronic state, in the bond lengths between Pu atoms, and in the density.

the trigonal strain needed to achieve the current value of α .

Figure 4 maps out the resulting hysteretic phase transitions between the ground state and the unpaired, metastable state. Both phases exhibit stability against small amounts of trigonal strain. The region of stability for the paired state spans a smaller change in α than that of the unpaired state: a trigonal distortion of the ground state to within a few degrees of the metastable state induces the transition; in the reverse direction, the metastable state must be pushed beyond the ground state at $\alpha=90^\circ$ to bring about the transition. In terms of energy, the paired state appears in a more stable well with a depth of 18 meV/atom compared to the 10 meV/atom of the unpaired state. These values suggest that experimental observation of the transitions would require temperatures well below room temperature.

It may be more convenient to not consider the strain as trigonal, but view it as uniaxial in the direction of the bond connecting paired Pu atoms. The predicted hysteresis then

stems from driving the system through the transition with uniaxial tension and uniaxial compression. In terms of lattice constants parallel and perpendicular to the pairing, the transitions occur at a ratio between 1.08 and 1.10 (paired into unpaired) and between 1.00 and 0.98 (unpaired into paired). The energy minimum of the unpaired state occurs at 1.14.

The structural phase transitions of elemental Pu have long been known to exhibit hysteresis in the temperature.³⁰ InPu thus would not be the first Pu system to exhibit hysteresis, but the simplicity of the pathway and its susceptibility to uniaxial strain make it appealing for further study. Experimental verification or refutation of the predictions would enhance the understanding of Pu's unique properties and the methods developed to address them.

Many thanks go to John Wills for helpful and encouraging discussions. This research is supported by the U.S. Department of Energy under Contract No. DE-AC52-06NA25396.

- ¹*The Chemistry of the Actinide Elements*, edited by L. R. Morss, N. M. Edelstein, and J. Fuger (Springer, Dordrecht, 2006).
- ²T. Lookman, A. Saxena, and R. C. Albers, *Phys. Rev. Lett.* **100**, 145504 (2008).
- ³S. P. Rudin, *Phys. Rev. Lett.* **98**, 116401 (2007).
- ⁴R. E. Peierls, *Quantum Theory of Solids* (Clarendon, Oxford, 1955).
- ⁵S. P. Rudin, *Phys. Rev. B* **76**, 195424 (2007).
- ⁶P. Hohenberg and W. Kohn, *Phys. Rev.* **136**, B864 (1964).
- ⁷F. H. Ellinger, C. C. Land, and K. A. Johnson, *Trans. Metall. Soc. AIME* **233**, 1252 (1965).
- ⁸W. Kohn and L. J. Sham, *Phys. Rev.* **140**, A1133 (1965).
- ⁹D. C. Langreth and J. P. Perdew, *Phys. Rev. B* **21**, 5469 (1980).
- ¹⁰B. Johansson, *Philos. Mag.* **30**, 469 (1974).
- ¹¹B. Johansson, *Phys. Rev. B* **11**, 2740 (1975).
- ¹²H. L. Skriver, O. K. Andersen, and B. Johansson, *Phys. Rev. Lett.* **41**, 42 (1978).
- ¹³S. Méot-Reymond and J. M. Fournier, *J. Alloys Compd.* **232**, 119 (1996).
- ¹⁴O. Eriksson, J. D. Becker, A. V. Balatsky, and J. M. Wills, *J. Alloys Compd.* **287**, 1 (1999).
- ¹⁵S. Y. Savrasov, G. Kotliar, and E. Abrahams, *Nature (London)* **410**, 793 (2001).
- ¹⁶A. V. Postnikov and V. P. Antropov, *Comput. Mater. Sci.* **17**, 438 (2000).
- ¹⁷Y. Wang and Y. Sun, *J. Phys.: Condens. Matter* **12**, L311 (2000).
- ¹⁸A. M. N. Niklasson, J. M. Wills, M. I. Katsnelson, I. A. Abrikosov, O. Eriksson, and B. Johansson, *Phys. Rev. B* **67**, 235105 (2003).
- ¹⁹P. Soderlind and B. Sadigh, *Phys. Rev. Lett.* **92**, 185702 (2004).
- ²⁰G. Robert, A. Pasturel, and B. Siberchicot, *Phys. Rev. B* **68**, 075109 (2003).
- ²¹G. Robert, C. Colinet, B. Siberchicot, and A. Pasturel, *Philos. Mag.* **84**, 1877 (2004).
- ²²B. Sadigh and W. G. Wolfer, *Phys. Rev. B* **72**, 205122 (2005).
- ²³J. C. Lashley, A. Lawson, R. J. McQueeney, and G. H. Lander, *Phys. Rev. B* **72**, 054416 (2005).
- ²⁴G. Kresse and J. Furthmüller, *Phys. Rev. B* **54**, 11169 (1996).
- ²⁵G. Kresse and D. Joubert, *Phys. Rev. B* **59**, 1758 (1999).
- ²⁶P. E. Blöchl, *Phys. Rev. B* **50**, 17953 (1994).
- ²⁷J. P. Perdew, J. A. Chevary, S. H. Vosko, K. A. Jackson, M. R. Pederson, D. J. Singh, and C. Fiolhais, *Phys. Rev. B* **46**, 6671 (1992).
- ²⁸J. P. Perdew, J. A. Chevary, S. H. Vosko, K. A. Jackson, M. R. Pederson, D. J. Singh, and C. Fiolhais, *Phys. Rev. B* **48**, 4978 (1993).
- ²⁹P. E. Blöchl, O. Jepsen, and O. K. Andersen, *Phys. Rev. B* **49**, 16223 (1994).
- ³⁰R. G. Liptai and R. J. Friddle, *J. Less-Common Met.* **10**, 292 (1966).